Journal of The Electrochemical Society, **155** (12) J361-J364 (2008)
0013-4651/2008/155(12)/J361/4/$23.00 © The Electrochemical Society

Effects of Hydrogen Plasma Treatment on Field-Emission Characteristics of Palladium Nanogap Emitters

Chih-Hao Tsai,[a] Kuan-Jung Chen,[a] Fu-Ming Pan,[a,z] Hsiang-Yu Lo,[b] Yiming Li,[b] Mei-Chao Chiang,[c] and Chi-Neng Mo[c]

[a]*Department Materials Science and Engineering and* [b]*Department Communication Engineering, National Chiao-Tung University, Hsinchu, Taiwan*
[c]*Chunghwa Picture Tubes, Limited, Taoyuan, Taiwan*

Nanogaps were prepared on the Pd line electrode by focused ion beam, and electron field-emission characteristics of the Pd nanogap emitter subject to hydrogen plasma treatment were studied. The as-prepared nanogap had smooth and uniform gap edges, and thus field-emission characteristics of the nanogap emitter were primarily dependent on the gap separation. After the hydrogen plasma treatment, the field-emission property of the Pd nanogap emitter was significantly enhanced. The improvement in the field-emission property was mainly attributed to formation of a ragged morphology on the nanogap emitter during the hydrogen plasma treatment. The ragged morphology provided more emitting sites with a high field enhancement factor. The Fowler–Nordheim plot was used to elucidate the dependence of field-emission characteristics of the Pd nanogap emitter on the plasma-induced ragged morphology.
 [DOI: 10.1149/1.2988646]

Manuscript submitted December 7, 2007; revised manuscript received August 31, 2008. Published October 8, 2008.

Electrodes with a nanometer-scale gap have many appealing applications, such as molecular electronics,[1,2] biomolecular detection,[3,4] and vacuum microelectronics.[5-7] However, because of the complexity and reliability of nanogap fabrication and integration, practical applications of most nanogap devices are still far beyond realization. Recent demonstration of a prototype surface conduction electron emission display (SED) is probably the one nanogap application having the greatest commercial potential and receiving the most attention in recent years.[8] The nanogap in a surface conduction electron emission (SCE) device of the SED display was fabricated on palladium oxide line electrodes deposited by ink-jet printing. To produce the nanogap, the PdO electrode was subject to a series of electrical forming and activation processes. Carbonaceous materials were required to be selectively deposited on the Pd electrode to further narrow down the nanogap to a width of 4–6 nm. Because of the complex fabrication processes, production of the SED display is costly and probably unreliable. In a previous study, we successfully fabricated a Pd nanogap field emitter with the gap separation of <30 nm by hydrogenation of Pd line electrodes.[9] The mechanistic principle of the Pd nanogap formation was based on the well-known phenomenon that hydrogen absorption in a Pd film can lead to hydride formation and hydride phase transformation, which will result in a compressive stress in the Pd film.[10] Presently, we are undertaking various approaches to improve field-emission characteristics of the Pd nanogap SCE device, including optimization of hydrogenation conditions and hydrogen plasma treatments. Earlier studies have shown that adsorption of hydrogen could enhance field-emission properties of electron field emitters.[11,12] In the study, we used hydrogen plasma to modify the Pd nanogap electrodes and studied improvements in field-emission properties of the nanogap emitter. The hydrogen plasma treatment could not only create a ragged morphology on the Pd nanogap emitter by ion bombardment but also could cause a work function lowering. Because using focused ion beam (FIB) to fabricate nanostructured patterns is a simple and reliable method, we used FIB in this study to prepare nanogaps with well-defined gap separations on the Pd line electrode instead of using the Pd hydrogenation process, which generally produces nanogaps with irregular edge shape. Field-emission characteristics of the FIB-prepared nanogap emitter could be significantly improved by the hydrogen plasma treatment.

Experimental

A schematic of the Pd thin-film emitter structure is shown in Fig. 1. The p-type (100) silicon wafer was used as the substrate. A SiO_2 layer 100 nm thick was first thermally grown on the Si substrate. The Pd line electrode was contacted with the underlying Pt/Ti pad electrodes. Before electron beam evaporation (E-beam) deposition of the Pt thin-film pad electrode (10 nm thick), the Ti layer (5 nm thick) was E-beam deposited on the oxide as an adhesion layer. A photolithographical liftoff process was used to pattern the Pt/Ti pad electrodes. The Pd thin-film strip (30 nm thick and 3 μm wide) was then E-beam deposited on the Pt/Ti pad electrode, and the strip pattern was also defined by the liftoff method. A FIB system (FEI Company) was used to prepare the nanogap on the Pd line electrode using a gallium ion source at a beam energy of 30 keV. The gap separation was controlled by tuning the ion beam current, and the achievable minimum gap separation in the study was ~25 nm. The surface of the Pd line electrode was modified by hydrogen plasma in a microwave plasma chemical vapor deposition system (ASTeX PDS-17) under the following treatment condition: microwave frequency, 2.45 GHz; power density, 124 W/cm^2; H_2 flow rate, 100 sccm; working pressure, 30 Torr; and substrate temperature, 300°C. The lattice constant of the Pd thin film before and after the plasma treatment was studied by a grazing incident X-ray diffractometer (Bede D1). Surface morphology was examined by scanning electron microscope [(SEM), JEOL 6500] and atomic force microscope (Veeco D5000). Field-emission properties of the Pd nanogap emitter were studied with a Keithley 237 source measurement unit under a vacuum condition of $\sim 5 \times 10^{-6}$ Torr.

Results and Discussion

The FIB prepared nanogap on the Pd thin-film line electrode had smooth gap edges and a uniform gap separation. The plane-view SEM images of the nanogaps with a gap separation of ~30 and ~90 nm are shown in Fig. 2a and b, respectively. From the top view, both the nanogaps had very similar morphological features, such as edge smoothness and uniformity. The rough feature shown on the side area of the Pd line electrode was likely a result of the liftoff lithography process. The photoresist pattern might disturb Pd deposition on the region near the edge of the Pd line electrode.

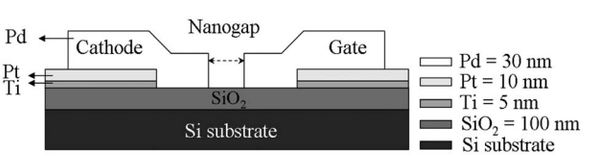

Figure 1. Schematic cross-sectional diagram of the palladium emitter structure.

[z] E-mail: fmpan@faculty.nctu.edu.tw

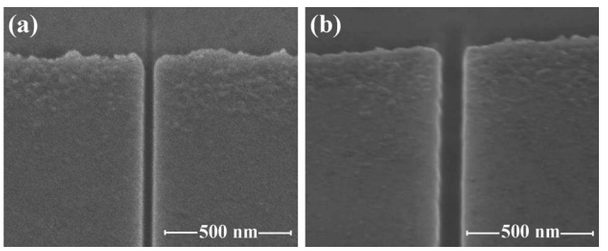

Figure 2. Plane-view SEM images of the FIB prepared Pd nanogaps with a gap separation of: (a) 30 and (b) 90 nm.

Because of the smaller gap separation, the nanogap with a 30 nm separation had a much better field-emission efficiency than the one with the 90 nm separation. Figure 3 shows the field-emission current of the two nanogap emitters as a function of the applied voltage [current-voltage (*I-V*) curve]. The dependence of the emission current of a field emitter on the applied voltage is described by the Fowler–Nordheim (F-N) relation

$$I = A\left(\frac{\alpha\beta^2}{\phi d^2}\right)V^2 \exp\frac{-B\phi^{3/2}d}{\beta V} \quad [1]$$

where V is the applied voltage, α is the emitting area, ϕ is the cathode work function, d is the distance between the cathode and anode (i.e., gate in the SCE device), β is the field enhancement factor, and A and B are generally considered as constants under a typical field-emission condition. The field enhancement factor β relates the applied voltage with the local electric field E_{loc} at the emitting site by the relation $E_{loc} = \beta(V/d)$ and is strongly dependent on the geometric shape of the field emitter. The insets in Fig. 3 are the corresponding F–N plots of the *I-V* curves. The linear feature of the F-N plots suggests that electron emission in the nanogap followed the F–N field-emission mechanism. From the F-N plot, the turn-on voltages (V_t) of the 30 and 90 nm nanogaps, which are herein defined as the bias voltage at which the F-N plot begins to exhibit a linear rising feature, were ~50 and ~125 V, respectively. According to Eq. 1, the slope of the F-N plot (S) is given by

$$S = \frac{-B\phi^{3/2}d}{\beta} \quad [2]$$

The F-N slopes of the 30 and 90 nm nanogaps were determined from Fig. 3 to be −245 and −1455, respectively. The measured slope

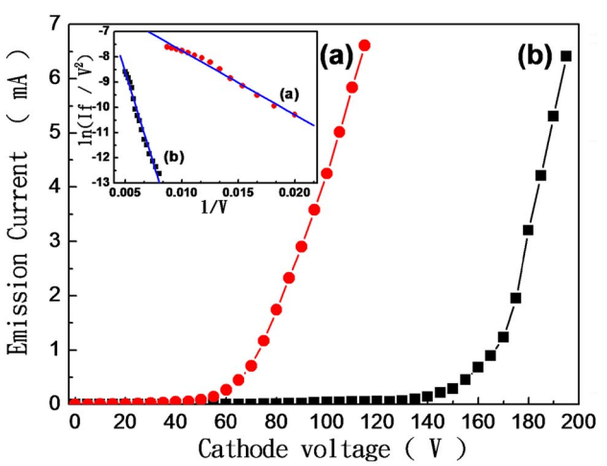

Figure 3. (Color online) Field-emission *I-V* curves and the corresponding F-N plots (inset) of the FIB prepared nanogap emitters with a gap separation of: (a) 30 and (b) 90 nm.

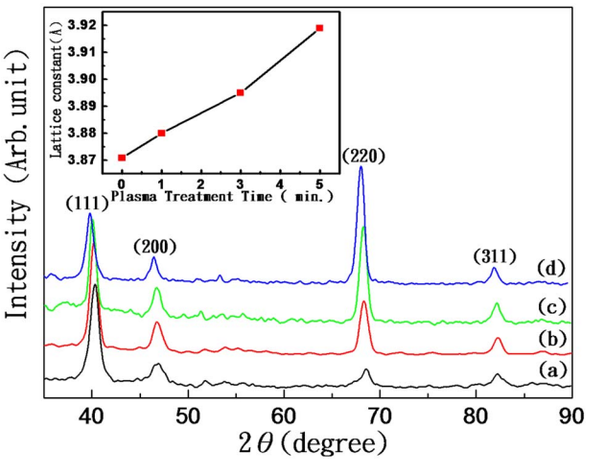

Figure 4. (Color online) XRD spectra of the Pd thin film as a function of hydrogen treatment time: (a) as-deposited, (b) 1, (c) 3, and (d) 5 min. The fcc lattice constant of the Pd thin films as a function of the plasma treatment time is shown in the inset.

of the 90 nm nanogap was about 6 times that of the 30 nm nanogap. Because the slope is linearly proportional to the nanogap separation and inversely proportional to the field enhancement factor, the 30 nm nanogap must have a β value twice that of the 90 nm nanogap.

Field-emission characteristics of the FIB-prepared nanogaps were significantly improved when the Pd line electrode was subject to the hydrogen plasma treatment, which could greatly modify the surface morphology and chemical composition of the Pd electrode. Because of the very small mass, hydrogen atoms can easily diffuse into the Pd lattice and occupy octahedral interstitial sites of the face-centered-cubic (fcc) lattice.[10,13] Hydrogen absorption in Pd is known to form two hydride phases, α and β phases, depending on the hydrogen concentration and the absorption temperature.[13] Phase transformation from the solid solution phase (α) to the interstitial compound phase (β) is accompanied by a lattice expansion and thus results in a large film stress. When the Pd thin film was subject to the hydrogen plasma treatment, hydrogen radicals in the plasma could be effectively absorbed in the Pd electrode, thereby forming the Pd hydride phases. Lattice expansion of the Pd electrode due to the hydride phase transformation was studied by X-ray diffraction (XRD) analysis. Figure 4 shows the XRD spectra of a blanket Pd thin film treated by the hydrogen plasma for various treatment times. The XRD spectrum of the as-deposited Pd thin film showed diffraction peaks from the (111), (200), (220), and (311) lattice orientations. The lattice constant, derived from Bragg's equation, of the as-deposited Pd thin film was 3.871 Å. As the plasma treatment time increased, all the diffraction peaks exhibited shifts toward lower diffraction angles, indicating an increase in the lattice spacing. The dependence of the (111) peak shift and the fcc lattice constant on the plasma treatment time is shown in the inset of Fig. 4. After the hydrogen plasma treatment of 5 min, the lattice constant increased from 3.871 to 3.919 Å, revealing that Pd hydride was formed in the Pd thin film.[10] It is interesting to note that the intensity of the (220) peak increased with the plasma treatment time. The increase of the (220) peak implied preferential texturing developed in the Pd electrode during the plasma treatment. Work function is a strong function of the crystal orientation. It has been reported that single crystalline Pd has work functions of 5.20, 5.65, and 5.95 eV for the (110), (100), and (111) orientations, respectively.[14] Therefore, field-emission characteristics of the Pd nanogap can vary with the change in the work function of the electron-emitting surface due to evolution of the preferential texturing in the electrode.

The surface morphology of the Pd electrode was significantly

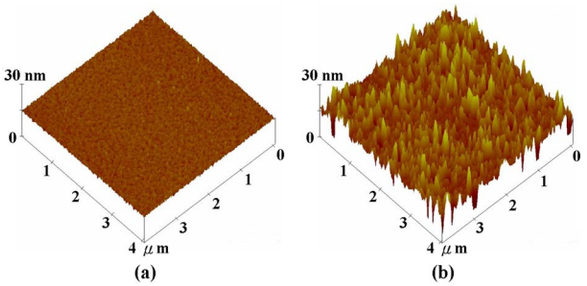

Figure 5. (Color online) AFM images of Pd thin films (a) before and (b) after the hydrogen plasma treatment of 5 min. The scanning area was 4 × 4 μm, and the height scale was 30 nm.

modified by the hydrogen plasma treatment. Figure 5 shows atomic force microscopy (AFM) images of a blanket Pd thin film before and after the hydrogen plasma treatment. The surface of the as-deposited Pd thin film was smooth as shown in Fig. 5a with a root-mean-square (rms) roughness of 0.66 nm. After the hydrogen plasma treatment, the film surface became very rough and the rms roughness increased with the plasma treatment time. The Pd film subject to the plasma treatment of 5 min had an rms roughness of ~7.30 nm (Fig. 5b). The SEM images of one of the gap edges of the 90 nm Pd nanogap before and after the plasma treatment of 5 min are shown in Fig. 6a and b, respectively. The SEM images show only one edge of the nanogap because the other side of the nanogap electrode was etched away by a FIB so that the sidewall edge of the nanogap could be clearly examined. Before the plasma treatment, the FIB-prepared nanogap had smooth gap edges. However, the edge of the 90 nm nanogap became jagged after the plasma treatment, and voids were even produced on the Pd electrode as shown in the plane-view SEM image of Fig. 6c. The development of the rugged morphology on the Pd electrode was likely due to hydrogen ion bombardment. Displacement of surface atoms and formation of vacancies could take place during hydrogen ion bombardment. Concurrent atom and vacancy migrations under the energetic plasma condition could lead to agglomeration of atoms and void formation on the Pd electrode, resulting in a surface of rugged microtopography. In addition, as described above, formation of the hydride phase during hydrogen plasma treatment could result in a compressive stress in the Pd electrode. If the stress was not distributed uniformly in the Pd line electrode because of defects and grain boundaries,

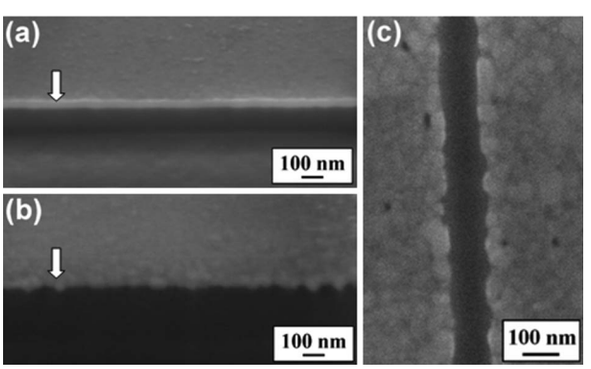

Figure 6. SEM images of the nanogap edge of the 90 nm nanogap emitter: (a) as-prepared and (b) after the hydrogen plasma treatment of 5 min, and (c) the plan-view SEM image of the Pd 90 nm nanogap emitter after the plasma treatment of 5 min. The SEM images of (a) and (b) show only one edge of the nanogap as marked by the arrows. A FIB was used to cut out a square crater on the substrate area, where the other side of the nanogap electrode was located, and therefore, only one sidewall edge can be observed.

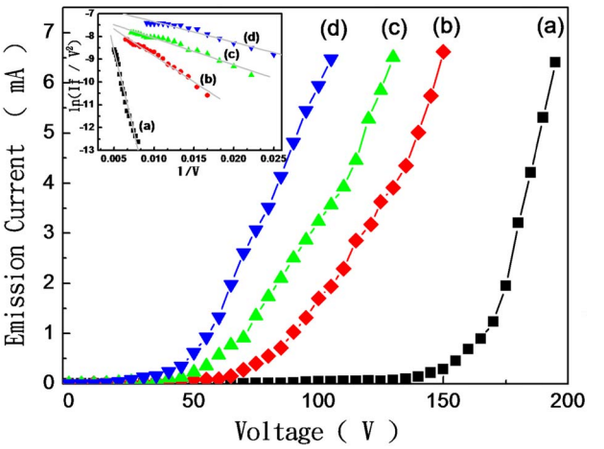

Figure 7. (Color online) Field-emission *I-V* curves of the 90 nm nanogap emitter after the hydrogen plasma treatment of various treatment times: (a) as-prepared, (b) 1, (c) 3, and (d) 5 min. The corresponding F-N plots are shown in the inset.

then it could enhance atom migration toward a less stressed area during the plasma treatment and, thus might play a non-negligible role in assisting surface roughening.[15]

Figure 7 shows field-emission *I-V* curves and the corresponding F-N plots of the 90 nm nanogap emitter subject to the hydrogen plasma treatment of various times. After the plasma treatment, the nanogap emitter showed a great improvement in field-emission properties. For the nanogap with the plasma treatment of 5 min, the turn-on voltage was ~40 V, which was even smaller than that of the as-prepared 30 nm nanogap, and a field-emission current as high as 2 mA was obtained at a bias of 65 V. The field-emission current increased significantly with the plasma treatment time. The F-N slopes of the nanogap emitters treated with the hydrogen plasma for 1, 3, and 5 min were −231, −118, and −90, respectively. Because the nanogaps exhibited a trivial change in the average gap separation after the plasma treatment, the plasma-treated nanogap emitters must have a larger field enhancement factor or a smaller work function as revealed by Eq. 2. Formation of Pd hydrides on a smooth Pd thin film by hydrogenation may result in either a small decrease or increase in the work function, depending on the hydrogen absorption temperature.[16,17] It was also reported that increase in film roughness could significantly reduce the work function of metallic thin films.[16,18] A work function reduction as large as 2 eV after hydrogen absorption in Pd at 78 K has been observed and mainly ascribed to the severe change in the Pd film morphology.[16] Therefore, it is likely that the larger rms roughness of the Pd nanogap emitters receiving a longer plasma treatment could induce a larger work function lowering and thus lead to a shallower F-N slope. We used a UV photoelectron spectroscope (RKI model AC-2) to measure work functions of the Pd thin film at 298 K. The work functions of the Pd thin film before and after the hydrogen plasma treatment for 5 min were 5.08 and 4.65 eV, respectively. According to Eq. 2, the slope of the F-N plot varies with the work function by a power of 3/2. If only the measured change in the work functions of the Pd thin film before and after the plasma treatment were taken into account, then the corresponding F-N slope should be decreased by just a factor of 1.14. Thus, the 16-fold decrease in the F-N slope suggested that the β value was increased by a factor of ~14 after the plasma treatment of 5 min, assuming no significant change in *d*, the nanogap separation. Therefore, the large increase in the β value was the predominant cause leading to the improvement in field-emission characteristics of the nanogap emitter after the plasma treatment.

As described above, the Pd nanogap emitter had a jagged edge and a rough surface after the plasma treatment. Under a negative

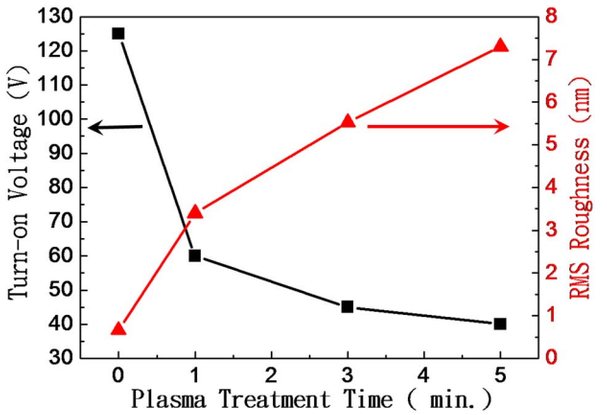

Figure 8. (Color online) The turn-on voltage and AFM rms roughness of the Pd nanogap emitter as a function of the hydrogen plasma treatment time.

bias, the local electric field at the emitting site with a rugged shape can be greatly enhanced, and thus field emission characteristics of the emitter are effectively improved. Figure 8 shows the dependence of the turn-on voltage and the rms roughness on the plasma treatment time. The turn-on voltage decreased with increasing the plasma treatment time. The most dramatic V_t drop from ~125 to ~ 60 V occurred to the nanogap treated by the hydrogen plasma of 1 min. Although further plasma treatment could reduce more the V_t, the nanogap exhibited a gradual V_t drop after the first minute of the plasma treatment. The rms roughness increased with the plasma treatment time and also had the greatest change for the first minute of the plasma treatment, but in a moderate way. According to the F-N plots shown in Fig. 7, the F-N slope showed a similar reduction behavior as well (i.e., the slope decreased most markedly in the first minute of the plasma treatment). The dramatic V_t and F-N slope reduction during the first minute of the plasma treatment seemed to suggest that most effective emission sites with a high field enhancement factor were created in the nanogap within the first minute of the plasma treatment, leading to a significant improvement on field-emission properties. Aside from creating emission sites, to prolong the plasma treatment could further modify the emitter surface, resulting in an increase in the emitting area and a decrease in the work function.

Conclusion

A FIB was used to prepared nanogaps on Pd line electrodes, and effects of the hydrogen plasma treatment on field-emission characteristics of the nanogap emitter were studied. The FIB-prepared nanogap was smooth and uniform on the gap edges, and therefore, the gap separation was the main fabrication parameter determining field-emission characteristics of the nanogap emitter. For the nanogap emitter with a gap separation of 30 nm, a turn-on voltage of 50 V was obtained. After the hydrogen plasma treatment, Pd hydrides were formed in the Pd nanogap emitter according to XRD analysis. The plasma-treated emitter had jagged nanogap edges and a very rough surface. Field-emission performance of the nanogap emitter was significantly improved after the plasma treatment. The turn-on voltage of the emitter decreased with increasing the plasma treatment time. The 90 nm nanogap emitter treated by hydrogen plasma for 5 min exhibited a lower turn-on voltage and a much higher field-emission current as compared to the 30 nm nanogap emitter without the plasma treatment. The improvement in the field-emission property was attributed to the ragged morphology of the nanogap emitter. The ragged morphology created more emitting sites and enhanced the local electric field. In addition, work function lowering was observed for the Pd thin film after the hydrogen plasma treatment, and the field-emission property of the nanogap emitter might thus be further improved.

Acknowledgments

This work was partly supported by the National Science Council of Taiwan, under contract no. NSC94-2120-M009-008 and Chunghwa Picture Tubes, Ltd. Technical supports from the National Nano Device Laboratories (NDL) is gratefully acknowledged.

National Chiao Tung University assisted in meeting the publication costs of this article.

References

1. M. A. Reed, C. Zhou, C. J. Muller, T. P. Burgin, and J. M. Tour, *Science*, **278**, 252 (1997).
2. A. Bezryadin and C. Dekker, *J. Vac. Sci. Technol. B*, **15**, 793 (1997).
3. C. C. Chen, J. T. Sheu, S. L. Chiang, and M. L. Sheu, *Jpn. J. Appl. Phys., Part 1*, **45**, 5531 (2006).
4. Y. Otsuka, Y. Naitoh, T. Matsumoto, W. Mizutani, H. Tabata, and T. Kawai, *Nanotechnology*, **15**, 1639 (2004).
5. H. I. Lee, S. S. Park, D. I. Park, S. H. Ham, J. H. Lee, and H. H. Lee, *J. Vac. Sci. Technol. B*, **16**, 762 (1998).
6. E. Yamaguchi, K. Sakai, I. Nomura, T. Ono, M. Yamanobe, N. Abe, and T. Hara, *J. Soc. Inf. Disp.*, **5**, 345 (1997).
7. H. Fujii, S. Kanemaru, H. Hiroshima, S. M. Gorwadkar, T. Matsukawa, and J. Itoh, *Appl. Surf. Sci.*, **146**, 203 (1999).
8. K. Yamamoto, I. Nomura, K. Yamazaki, S. Uzawa, and K. Hatanaka, *SID Symp. Digest*, **36**, 1933 (2005).
9. C. H. Tsai, K. J. Chen, F. M. Pan, M. Liu, and C. N. Mo, *Appl. Phys. Lett.*, **90**, 163115 (2007).
10. F. A. Lewis, *The Palladium/Hydrogen System*, pp. 13–49, 94–117, Academic Press, London (1967).
11. B. R. Chalamala and R. H. Reuss, *Appl. Phys. Lett.*, **78**, 2967 (2001).
12. B. R. Chalamala, R. M. Wallace, and B. E. Gnade, *J. Vac. Sci. Technol. B*, **16**, 2855 (1998).
13. E. Wicke and H. Brodowsky, in *Hydrogen in Metals II*, G. Alefeld and J. Völkl, Editors, pp. 73–155, 305–330, Springer-Verlag, Berlin (1978).
14. K. Wandelt, in *Thin Metal Films and Gas Chemisorption*, P. Wissmann, Editor, p. 200, Elsevier, Amsterdam (1987).
15. C. J. Zhai and R. C. Blish, *J. Appl. Phys.*, **97**, 113503 (2005).
16. R. Du's, R. Nowakowski, and E. Nowicka, *J. Alloys Compd.*, **404–406**, 284 (2005).
17. R. Du's and E. Nowicka, *Langmuir*, **16**, 584 (2000).
18. W. Li and D. Y. Li, *J. Chem. Phys.*, **122**, 064708 (2005).